

Representation Learning of Lab Values via Masked AutoEncoder

David Restrepo *

*Massachusetts Institute of Technology (MIT), USA
Université Paris-Saclay, France*

Chenwei Wu*

University of Michigan, USA

Yueran Jia

Northeastern University, USA

Jaden K. Sun

Massachusetts Institute of Technology (MIT), USA

Jack Gallifant

*Harvard Medical School, USA
Brigham and Women's Hospital/Dana-Farber Cancer Institute, USA*

Catherine G. Bielick

*Massachusetts Institute of Technology (MIT), USA
Harvard Medical School, USA
Beth Israel Deaconess Medical Center, USA*

Yugang Jia

Massachusetts Institute of Technology (MIT), USA

Leo A. Celi

*Massachusetts Institute of Technology (MIT), USA
Harvard Medical School, USA
Beth Israel Deaconess Medical Center, USA*

LEOANTHONYCELI@YAHOO.COM

Abstract

Accurate imputation of missing laboratory values in electronic health records (EHRs) is critical to enable robust clinical predictions and reduce biases in AI systems in healthcare. Existing methods, such as variational autoencoders (VAEs) and decision tree-based approaches such as XGBoost, struggle to model the complex temporal and contextual dependencies in EHR data, mainly in underrepresented groups. In this work, we propose Lab-MAE, a novel transformer-based masked autoencoder framework that leverages self-supervised learning for the imputation of continuous sequential lab values. Lab-MAE introduces a structured encoding scheme that jointly models laboratory test values and their corresponding timestamps, enabling explicit capturing temporal dependencies. Empirical evaluation on the MIMIC-IV dataset demonstrates that Lab-MAE signifi-

cantly outperforms the state-of-the-art baselines such as XGBoost across multiple metrics, including root mean square error (RMSE), R-squared (R²), and Wasserstein distance (WD). Notably, Lab-MAE achieves equitable performance across demographic groups of patients, advancing fairness in clinical predictions. We further investigate the role of follow-up laboratory values as potential shortcut features, revealing Lab-MAE's robustness in scenarios where such data is unavailable. The findings suggest that our transformer-based architecture, adapted to the characteristics of the EHR data, offers a foundation model for more accurate and fair clinical imputation models. In addition, we measure and compare the carbon footprint of Lab-MAE with the baseline XGBoost model, highlighting its environmental requirements.

* These authors contributed equally

Data and Code Availability The code to reproduce our experiments is available in [github](#). The data set used is also publicly available¹

1. Introduction

Laboratory values play a pivotal role in real-time clinical care by demonstrating a patient’s baseline physiology, generating a differential diagnosis for acute or chronic illnesses, and guiding prognosis. The effectiveness of machine learning (ML) models in leveraging laboratory data from electronic health records (EHRs) is often hampered by the prevalence of missing values [Luo \(2022\)](#); [Austin et al. \(2021\)](#), which can severely affect model performance and introduce harmful bias in clinical implementation [Riley et al. \(2024\)](#). In addition to technical challenges, the social patterning inherent in the data generation, often drives missing data in clinical datasets. Factors such as socioeconomic status, access to healthcare, and systemic biases can significantly influence the availability of laboratory results, affecting underrepresented groups and introducing skew into clinical datasets [Teotia et al. \(2024\)](#). Optimal handling of missing data in this context is a critical challenge, as it directly affects the reliability of clinical models in healthcare settings.

Conventional imputation techniques, such as mean and standard deviation-based substitutions, are not well-suited to clinical tasks due to highly contextualized and individualized interpretation. These simplistic approaches fail to capture the intricate temporal and inter-variable dependencies present in high-dimensional physiological data [Li et al. \(2021\)](#). For example, the clinical importance of high Creatinine values in the hospitalized setting depends heavily on the patient’s own baseline values and the presence of any of the potential causes of acute kidney injury, including sepsis, hemorrhage, iatrogenic causes, urinary tract obstruction, and more. Some advanced methods, such as training multiple tabular models such as XGBoost [Chen and Guestrin \(2016\)](#) for individual lab values, have been used to capture these data relations in lab values [Zhang et al. \(2020\)](#); [Chen and Guestrin \(2016\)](#). However, even these models often struggle to fully leverage the available information, leading to suboptimal solutions that may overlook

valuable contextual details [Waljee et al. \(2013\)](#); [Luo et al. \(2016\)](#).

Recent advances in self-supervised learning have opened new avenues for handling missing data by learning robust representations from the available data itself. Previous work on data imputation in EHR datasets has predominantly employed Variational Autoencoders (VAE) [Kingma \(2013\)](#) due to their ability to model latent distributions and generate plausible imputations [Zamanzadeh et al. \(2021\)](#). However, recent studies have shown that Masked Autoencoders (MAEs) offer notable improvements over VAEs, particularly in their ability to reconstruct high-dimensional data with fewer assumptions on the latent space and greater capacity to learn complex feature dependencies directly from the data [He et al. \(2022\)](#); [Bao et al. \(2021\)](#). These advances highlight the potential of MAEs to deliver more accurate and context-aware imputations for clinical data, motivating the development of our proposed framework.

In addition, transformer-based models have shown promise in fields such as natural language processing [Devlin \(2018\)](#); [Vaswani \(2017\)](#); [Renc et al. \(2024\)](#) and computer vision [Dosovitskiy \(2020\)](#); [Parvaiz et al. \(2023\)](#) due to their ability to model complex patterns and relationships within the data. Despite all the performance and results shown by transformer models in fields such as computer vision and natural language processing, the creation of foundation models and the training of transformer models for tabular data is a field that still needs to be further explored [van Breugel and van der Schaar \(2024\)](#). Some recent previous works have shown that deep learning models can improve classical models such as XGBoost [Chen and Guestrin \(2016\)](#) on tabular data tasks [Kadra et al. \(2021\)](#). Additionally, attention-based methods have demonstrated significant promise in tabular data imputation [Lee and Kim \(2023\)](#); [Wu et al. \(2020\)](#). [Kowsar et al. \(2024\)](#) proposed an attention-based missing value imputation framework that leverages self-attention and between-sample attention mechanisms to reconstruct missing data. Their method surpasses classical machine learning approaches, such as decision-tree-based imputation, and achieves superior performance on several EHR datasets. The potential of self-supervised pretraining for clinical data is immense, especially when combined with the transformer architecture, and techniques such as masked autoencoding, which aim to learn from the inherent structure of the data

1. This paper uses the MIMIC-IV dataset ([Johnson et al., 2023](#)), which is available in the PhysioNet repository ([Johnson et al., 2020](#)).

rather than relying on predefined labels He et al. (2022); Krishnan et al. (2022).

Building on this concept, LABRADOR, a novel continuous Transformer model, was designed to model laboratory data by using masked language modeling (MLM) techniques Bellamy et al. (2023). Despite LABRADOR’s innovative architecture and its success in capturing continuous lab data patterns, it still faced challenges in consistently outperforming traditional tree-based methods like XGBoost across various downstream tasks. This is in line with a broader body of evidence indicating that deep learning methods often underperform compared to tree-based techniques on tabular data due to a lack of appropriate inductive biases Grinsztajn et al. (2022).

Our proposed solution builds on the LABRADOR and ReMasker frameworks Du et al. (2023), introducing a novel masked autoencoder architecture tailored to the unique characteristics of laboratory data. By extending the principles of masked modeling to impute missing values and leveraging temporal information explicitly, our approach addresses the limitations observed in prior methods. Unlike conventional models, our architecture takes timestamps into account, which is critical for clinical data where the sequence of events can significantly influence outcomes.

The main contributions of this paper are as follows:

1. We develop and validate a masked autoencoder transformer model specifically designed for imputing missing lab values in EHR data, incorporating temporal and contextual information to enhance imputation accuracy.
2. We demonstrate that our model not only outperforms state-of-the-art tree-based methods, such as XGBoost, in the context of clinical data imputation but also mitigates biases by providing consistent performance across different patient demographics.
3. We introduce a self-supervised pre-training strategy that effectively learns high-dimensional representations of lab data, paving the way for more robust downstream predictions even in the absence of complete data.

Our approach combines the strengths of masked autoencoding with the Transformer architecture to create a powerful tool for handling missing lab values in clinical datasets. This advancement has the potential to significantly improve the quality and com-

pleteness of EHR data, ultimately enhancing clinical decision-making and patient outcomes.

2. Methods

2.1. Datasets

The dataset used in this study is derived from the MIMIC-IV database Johnson et al. (2020, 2023), which contains de-identified health records of patients admitted to critical care units at the Beth Israel Deaconess Medical Center between 2008 and 2019. Our focus was on the top 100 most common lab values, selected based on their occurrence in patient records. The cohort comprises data of 1,417,738 stays for training and 100,000 stays for evaluation. These cohorts were extracted and processed using Google BigQuery.

2.2. Data Processing

We utilized SQL queries through Google BigQuery to extract lab event data from the labevents table of MIMIC-IV Johnson et al. (2020, 2023). The data includes unique hospital admission IDs (hadm_id), patient race information for a further fairness and bias evaluation, lab test item IDs (itemid), lab test timestamps (charttime), and corresponding numerical lab values (valuenum). The dataset was preprocessed to remove invalid lab values (e.g., negative values) and filtered to include only valid, positive measurements.

For each patient admission, the earliest recorded timestamp for each lab test was used as a reference point. Additional columns were computed to represent the difference between each lab test’s timestamp and this reference. The numerical lab values were then normalized using quantile normalization to limit extreme outliers.

We also calculated follow-up values for each lab test (denoted as npval_last_id) by tracking subsequent tests performed within the same admission. For each lab test and follow-up, a corresponding time difference column was generated (denoted as nptime_id), representing the time elapsed since the reference point. The extracted data was further partitioned into training and test sets based on the timestamp, with admissions prior to the year 2179 used for training and those afterward for testing to avoid data leakage during evaluation.

The data preprocessing resulted in a train set of 1,417,738 rows used for training and an independent test set of 100,000 rows. Each dataset contains 3

Columns representing the patient ID, patient admission ID, and Patient’s race, as patient indicators. The dataset also contains 200 columns indicating the 100 lab values used and the time stamps, and other extra 200 columns for the follow-up values and timestamps. If the values are missing, those values were indicated using a Not a Number (NaN) value.

2.3. Foundation Lab-MAE Architecture

We base our foundation laboratory imputation model (Lab-MAE) on a Masked Autoencoder architecture, inspired by the Remasker framework [Du et al. \(2023\)](#). This architecture utilizes a Transformer backbone to capture complex correlations between lab values over time, providing robust imputation of missing data in medical records. The model is composed of an encoder-decoder structure that is trained in a self-supervised manner by masking portions of the input and reconstructing the masked values.

The model uses learned positional encodings to represent the unique lab IDs, and timestamps ensuring that each lab value and timestamp is always passed to the model in the same positional slot in the input sequence. This approach allows the model to consistently interpret each lab test and time, regardless of missing values or the presence of other tests. Specifically, the lab values are placed in predefined positions, and the timestamps corresponding to those lab tests are placed in the following position. This design enables the model to capture temporal relationships between the lab values and their corresponding times.

In this sense, let $x \in \mathbb{R}^{L \times d}$ represent the input sequence, where L is the sequence length (including both lab values and timestamps) and d is the embedding dimension of each token. The learned positional encodings $P \in \mathbb{R}^{L \times d}$ are added to the input sequence as follows:

$$z_0 = x + P \quad (1)$$

where z_0 is the input to the encoder. Positional encodings align lab values with corresponding timestamps, capturing temporal relationships.

Then, the encoder consists of multiple layers of Transformer blocks, where each block includes multi-head self-attention and feed-forward layers. The self-attention mechanism is defined as in the original ”attention is all you need” paper [Vaswani \(2017\)](#):

$$\text{Attention}(Q, K, V) = \text{softmax} \left(\frac{QK^T}{\sqrt{d_k}} \right) V \quad (2)$$

where Q , K , and V represent the query, key, and value matrices, respectively, and d_k is the dimensionality of the key vectors. To address the specific challenge of missing values in our dataset, we introduce a **missing value attention mask**, which prevents missing values from influencing the attention computation. Let $M \in \{0, 1\}^{L \times L}$ represent the attention mask, where $M_{ij} = 0$ indicates a missing value, and the corresponding attention score is masked out:

$$\tilde{A}_{ij} = \begin{cases} A_{ij}, & \text{if } M_{ij} = 1 \\ -\infty, & \text{if } M_{ij} = 0 \end{cases} \quad (3)$$

The decoder reconstructs the masked values by aggregating learnable masked tokens in the masked positions from the latent representation generated by the encoder. To ensure that missing values do not bias the model’s predictions, we introduce modifications to the loss function. Specifically, the reconstruction loss is only calculated for observed values (current and masked values), while missing values are ignored. Given the predicted values \hat{x} and true values x , the loss function L is defined as:

$$L = \frac{1}{\sum_i (1 - m_i)} \sum_{i=1}^L (1 - m_i) \cdot (\hat{x}_i - x_i)^2 \quad (4)$$

where m_i is the missingness indicator for each value. This ensures that the model focuses on reconstructing only the available data, and prevents the overfitting to missing values.

2.4. Lab-MAE Training

The Lab-MAE model was trained using a self-supervised learning approach with a focus on imputing missing values in clinical lab data. The training process involved several stages, including data preprocessing, model setup, optimization, and evaluation, designed to maximize the model’s ability to predict missing lab values from the MIMIC-IV dataset [Johnson et al. \(2020, 2023\)](#).

Before training, the dataset underwent to a preprocessing to handle missing values and remove irrelevant or redundant data points. Rows with fewer than 17 non-missing lab and time values were excluded from the training set. The remaining data

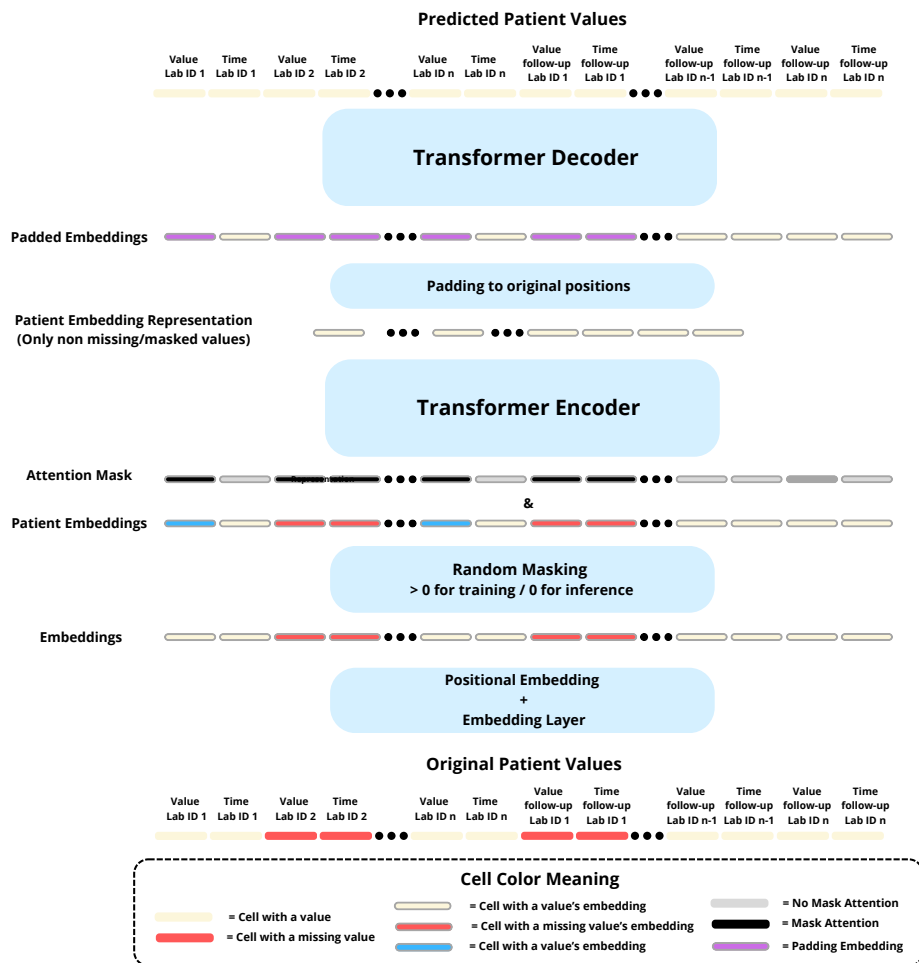


Figure 1: Foundation Lab-MAE training structure.

was normalized using a feature-wise min-max scaling technique to standardize the lab values across patients, enhancing the stability and convergence of the training process.

The Lab-MAE model was configured with the following hyperparameters: a hidden embedding dimension of 64, 8 layers for both the encoder and decoder, and 8 attention heads per layer. The model was trained with a mask ratio of 0.25, meaning that 25% of the input values were randomly masked during training to simulate missing data. A batch size of 256 was used to ensure efficient training, and the training was carried out for a maximum of 500 epochs. A checkpoint mechanism was implemented to save model weights at regular intervals, allowing the model to be resumed from any epoch if necessary.

The optimization of the model was handled using the AdamW optimizer, which is well-suited for training Transformer-based architectures due to its effective weight decay mechanism. The learning rate was initially set using a base learning rate scaling rule, proportional to the batch size. During training, a cosine annealing schedule was employed to adjust the learning rate dynamically. Specifically, the learning rate was warmed up linearly over the first 20 epochs, after which it followed a half-cycle cosine decay pattern, gradually reducing towards a specified minimum learning rate.

The model’s training objective was to minimize the Mean Squared Error (MSE) between the predicted and actual lab values, calculated only over the non-masked (observed) entries as shown in the equation 4.

The model was evaluated constantly on a validation set extracted from the training set. The validation was performed at regular intervals, with predictions assessed on standard additional metrics such as Root Mean Squared Error (RMSE), R-squared (R^2), Mean Absolute Error (MAE), and Wasserstein Distance (WD). The validation results were logged after every 30 epochs to monitor the model’s performance. Additionally, checkpointing enabled the continuous saving of the model’s state, allowing for the resumption or rollback of training to optimize performance based on the evaluation metrics.

This structured training approach enabled the model to learn robust representations of the temporal and contextual relationships between lab values, ultimately enhancing its ability to accurately impute missing values in the dataset and learn representations of the lab values.

2.5. Lab-MAE Imputation Evaluation

2.5.1. BASELINE MODELS

To benchmark the performance of our proposed foundation Lab-MAE model for lab value imputation, we implemented a set of baseline models using XGBoost. XGBoost was selected for its well-known capabilities in handling tabular data tasks, including its ability to directly manage missing values without requiring extensive preprocessing. A total of 100 separate XGBoost models, value were trained, one for each lab value, to provide a robust comparison against our foundation Lab-MAE model.

The training of these XGBoost models involved a hyperparameter optimization process using GridSearchCV to identify the best-performing configuration for each lab-specific model. The hyperparameter search was conducted using the following grid: Learning rate: [0.01, 0.1, 0.2], Max depth: [3, 4, 5], Number of estimators: [50, 100, 200].

GridSearchCV was applied with three-fold cross-validation to evaluate different parameter combinations, aiming to minimize the MSE of the lab value of interest. After identifying the optimal hyperparameters, each model was retrained using the entire training dataset to ensure the best possible predictive performance.

These trained XGBoost models served as our baseline for comparison with the Lab-MAE model. The key objective was to leverage XGBoost’s capability in handling missing data and its structured tree-based

learning mechanism to predict individual lab values based on the contextual data.

2.5.2. FOUNDATION LAB-MAE MODEL VS. XGB EVALUATION SETUP

Both the Lab-MAE and XGBoost models were evaluated using a cohort of 100,000 data points extracted from our independent test set. To ensure a fair comparison, the same data points were used across both models during evaluation. We computed three primary metrics for each lab value: RMSE, R^2 , and the WD. The R^2 metric was used as the main reference due to its ability to assess the correlation strength and its capacity to avoid overfitting to mean or most common values. The WD was used to assess how well the model captures the overall distribution of lab values, including extreme values, unlike RMSE and R^2 , which emphasize overall accuracy and variance explained. WD complements RMSE and R^2 by highlighting the quality of predictions in capturing not only central tendencies but also the full range of values, particularly the extremes. More information about the metrics is available in appendix A.

2.5.3. TEST SET EVALUATION PROCESS

The evaluation was conducted lab-by-lab to ensure comprehensive and robust performance assessment. For each lab value, we simulated missing data by masking its existing values in the test dataset, effectively challenging the models to predict these masked values using the remaining available context, including other lab values and the associated timestamps.

During inference with the Lab-MAE model, we ensured that no gradients were calculated, and the random masking ratio was set to zero, focusing purely on the prediction task.

Similarly, the XGBoost models were applied in a lab-specific manner, where each lab’s missing values were predicted using the corresponding XGBoost model trained for that specific lab. This approach allowed the XGBoost models to leverage their tree-based structure to effectively utilize the available data for predictions.

2.6. Fairness and Bias Analysis

The fairness and bias analysis in our study aimed to evaluate how well the Lab-MAE model performs across different demographic groups, particularly focusing on racial differences, and to assess the impact

of follow-up data as a potential shortcut feature in the imputation process.

2.6.1. LAB-MAE MODEL FAIRNESS ACROSS RACE GROUPS

To ensure that the Lab-MAE model’s predictions are equitable across different racial groups, we conducted an analysis of its performance for five race groups: White, Black, Hispanic, Asian, and Others. We compared the performance of the Lab-MAE model with the baseline XGBoost models for each race group using the same metrics.

For each race, the imputation model’s performance was calculated by comparing the predicted values to the actual lab values, using the following approach:

- Filter the test dataset to include only the records for the race group being evaluated.
- Mask the lab values to simulate missing data and use the Lab-MAE model to predict these values.
- Calculate the metrics WD, RMSE, and R^2 for each lab value to quantify the model’s prediction performance for the respective race group.

The results were consolidated into a single dataframe to allow a comparative analysis of the model’s fairness across racial categories.

2.6.2. CARBON FOOTPRINT MEASUREMENT

We assessed the carbon footprint of the Lab-MAE and baseline XGBoost models using the CodeCarbon library [Courty et al. \(2024\)](#). Emissions were estimated during the inference process for batch sizes of 1, 32, and 64 across multiple geographic locations, including Colombia, USA, France, Uganda, Philippines, and Australia. These locations were chosen to represent diverse geographic profiles in Asia, Africa, North America, South America, Europe, and Australia.

The models were evaluated by performing inference on subsets on the test dataset comparing the performance of the Lab-MAE model vs the set of XGBoost models. For each location, emissions were measured using simulated conditions based on the country’s emission factor, reflecting the environmental impact of running machine learning models in different parts of the world.

More details about the methodology used to calculate carbon emissions can be found in [Appendix B](#).

3. Results

3.1. Comparison of Lab-MAE vs. XGBoost for Data Imputation

In this section, we present the results of our comparison between the Lab-MAE and XGBoost models for the task of data imputation, evaluated using three metrics: WD, RMSE, and R^2 . These metrics were calculated on the entire set of 100 lab values and also on the top 20 most frequently occurring lab values to provide a more focused analysis.

3.1.1. OVERALL ANALYSIS OF ALL LAB VALUES

The comparison between the Lab-MAE and XGBoost models across all 100 lab values demonstrates that the Lab-MAE generally outperforms XGBoost. The average performance metrics calculated over the entire dataset indicate a lower WD and RMSE for the Lab-MAE model, and higher R^2 values, suggesting that the Lab-MAE model has a better predictive capability and is less prone to error.

Table 1: Comparison of Lab-MAE and XGBoost across evaluation metrics for the 100 lab values. Each column indicates the amount of values the model is outperforming, where 100 means that a model outperforms in all the lab values for certain metric.

Metric	Better Performer Lab-MAE (%)	Better Performer XGBoost (%)
RMSE	89	11
R^2	89	11
Wasserstein Distance	79	21

As shown in [Table 1](#), the comparison of Lab-MAE and XGBoost models across individual lab values provides a more nuanced evaluation of their performance. Instead of relying on mean values, which can obscure differences due to varying scales across lab tests, we analyze the number of lab values where each model performs better.

For WD, which evaluates the similarity between predicted and actual distributions (lower is better), Lab-MAE outperforms XGBoost in 79 out of 100 cases, demonstrating its superior ability to capture the underlying distributions, including extreme values.

For RMSE and R^2 , Lab-MAE achieves better performance in 89 cases, highlighting its robust-

ness in minimizing overall error magnitude and better variance-capturing capabilities compared to XGBoost which outperforms Lab-MAE only in 11 cases.

Although XGBoost managed to surpass Lab-MAE in 11 cases for RMSE and R^2 , and 21 cases for WD, these instances were relatively isolated. This suggests that while XGBoost can occasionally outperform Lab-MAE in specific scenarios, the Lab-MAE model exhibits more stable and reliable performance across a broader range of laboratory values.

3.1.2. FOCUSED ANALYSIS ON THE TOP 20 LAB VALUES

To provide a clearer understanding of the models' performance on the most relevant lab values, we analyzed the top 20 most frequently occurring lab values. This focused analysis highlights the significant differences in prediction accuracy between Lab-MAE and XGBoost for these high-impact features.

Table 2 illustrates the detailed performance metrics for both models on the top 20 most popular lab values. The Lab-MAE model consistently demonstrates superior performance, achieving lower RMSE and WD values, as well as higher R^2 scores for most lab values.

For example, for Creatinine, the Lab-MAE model achieved an RMSE of 0.233 compared to 0.261 for XGBoost, indicating a significant reduction in the average error. Furthermore, the WD for Lab-MAE was 0.034, which is lower than the 0.039 obtained by XGBoost. The R^2 score for Lab-MAE was 0.943, outperforming XGBoost's 0.929, demonstrating a stronger predictive capability.

This trend is not isolated to Creatinine; similar patterns are observed across other lab values. For Sodium, Lab-MAE showed a reduction in RMSE from 1.035 to 0.883 and in WD from 0.309 to 0.220, with an improvement in R^2 from 0.921 to 0.943, highlighting the model's robustness in reducing both large and small prediction errors.

In some cases, such as lab Platelet Count, both models presented challenges due to the complexity of the predictions. Nevertheless, Lab-MAE still showed slight improvements, with an RMSE of 39.861 versus 41.464 for XGBoost and an WD of 7.568 compared to 9.349. The R^2 values for this lab remained relatively high for both models, with Lab-MAE marginally outperforming XGBoost (0.866 versus 0.855).

The detailed comparison provided in Table 2 underscores the strengths of the Lab-MAE model, sug-

gesting that its ability to leverage the temporal and contextual information encoded in the dataset is a significant advantage over the XGBoost approach. These findings validate the hypothesis that a Transformer-based architecture, when properly trained and fine-tuned, can substantially improve data imputation tasks over classical machine learning methods.

The analysis confirms that the Lab-MAE model not only performs better overall but also excels particularly in the top 20 most frequently ordered lab values, making it a superior choice for data imputation tasks in clinical settings.

3.2. Fairness Analysis Across Race Groups

To gain deeper insights into the bias and fairness of the Lab-MAE and XGBoost models, we conducted a focused analysis on the top 20 most frequently occurring lab values, evaluating their performance across different racial groups. This detailed analysis reveals notable patterns in how each model performs for specific lab values, highlighting both strengths and potential biases.

Table 8, 9, and 10 available in Appendix E, illustrate the R^2 , WD, and RMSE values respectively of the Lab-MAE model across different racial groups for the top 20 lab values. The analysis reveals that the model's performance varies significantly depending on both the lab value and the racial group, indicating potential biases that warrant further attention.

One notable pattern is the consistent higher performance of the Lab-MAE model for Asian and White groups in certain lab values, which indicates a disparity in the model performance. This disparity in the performance is dependent on the lab value and metric used, highlighting the need of multiple metrics and domain specific metrics.

3.3. Carbon Footprint Results

After running experiments on inference of the Lab-MAE model versus the XGBoost models in batches of 1, 32 and 64 data points, and collecting the results, we averaged across six geographic locations spanning Asia, Africa, Australia, Europe, North America, and South America. Table 3 shows the mean values of duration, emissions, emissions rate, CPU power, GPU power, and RAM power for each model and batch size. Overall, Lab-MAE shows lower or comparable carbon footprints, particularly at lower batch sizes, whereas XGBoost sometimes demands a higher CPU

Table 2: Comparison of RMSE, WD, and R^2 between XGBoost and Lab-MAE models for top 20 most popular lab values.

Lab ID	RMSE (XGBoost)	RMSE (Lab-MAE)	WD (XGBoost)	WD (Lab-WD)	R^2 (XGBoost)	R^2 (Lab-MAE)
Creatinine	0.261	0.233	0.039	0.034	0.929	0.943
Hematocrit	0.579	0.564	0.046	0.040	0.989	0.989
Potassium	0.327	0.270	0.127	0.095	0.494	0.654
Sodium	1.035	0.883	0.309	0.220	0.921	0.943
Urea Nitrogen	4.910	4.531	0.750	0.540	0.913	0.925
Chloride	1.049	0.876	0.310	0.229	0.952	0.967
Bicarbonate	0.959	0.769	0.305	0.199	0.927	0.953
Anion Gap	1.008	0.808	0.356	0.208	0.872	0.918
Platelet Count	41.464	39.861	9.349	7.568	0.855	0.866
Hemoglobin	0.093	0.080	0.025	0.026	0.998	0.998
White Blood Cells	2.034	1.935	0.551	0.461	0.757	0.780
MCHC	0.194	0.114	0.035	0.027	0.982	0.994
Red Blood Cells	0.044	0.035	0.005	0.004	0.996	0.997
MCV	0.518	0.401	0.243	0.238	0.993	0.996
MCH	0.159	0.109	0.030	0.029	0.995	0.998
RDW	0.579	0.549	0.084	0.073	0.931	0.938
Glucose	30.392	29.277	11.667	10.095	0.426	0.468
Magnesium	0.184	0.178	0.079	0.071	0.457	0.491
Calcium, Total	0.342	0.324	0.097	0.082	0.691	0.723
Phosphate	0.536	0.511	0.187	0.155	0.615	0.650

power usage given the need of requiring a model per feature. These results provide insight into the energy efficiency of each model under different workload configurations.

As shown, Lab-MAE tends to have a shorter average duration (especially with smaller batch sizes), resulting in generally lower carbon emissions. XGBoost, although sometimes requiring lower CPU power, demonstrates higher total duration in the same scenarios, which contributes to a higher overall emissions rate. The duration is mainly because Lab-MAE is a single model, while XGBoost requires a model per lab value. These observations suggest that Lab-MAE may be more energy-efficient when deployed at scale since is a single foundation model.

4. Discussion

Our study introduces Lab-MAE, a novel transformer-based architecture that fundamentally advances the field of clinical data imputation while maintaining algorithmic fairness. Through an extensive empirical evaluation of the MIMIC-IV dataset [Johnson et al. \(2020, 2023\)](#), we demonstrate that Lab-MAE achieves superior performance compared to traditional approaches and exhibits remarkable consistency between demographic groups - a critical consideration for healthcare applications.

4.1. Clinical and Technical Implications

Our LAB-MAE demonstrates a greater ability to learn real-world distributions, which may be multipolar or characterized by extreme values. This is highlighted by consistent R^2 above XGB but reduced EMD/Wasserstein values overall and across subgroups. The model’s performance stability across demographic groups challenges the expected trade-off between accuracy and fairness in machine learning systems. This suggests that architectural innovations focused on capturing temporal and contextual relationships can simultaneously advance both objectives.

Another critical advantage of Lab-MAE lies in its design as a single foundation model capable of processing complex sequences of data, as opposed to the XGBoost approach that requires a separate model for each feature. This structural difference not only contributes to an improved energy efficiency, but also makes it a more scalable and practical solution for real-world applications.

4.2. Fairness and Equity Considerations

Previous approaches to laboratory value imputation have largely relied on traditional machine learning methods or simplified time-series models. Our model builds upon recent work by [Bellamy et al. \(2023\)](#) for modeling laboratory data, and [Du et al. \(2023\)](#) with the ReMasker framework for tabular data imputa-

Table 3: Carbon footprint of Lab-MAE and XGBoost under different batch sizes. Values represent the *average calculation using the mean* of the six geographic locations in South America, North America, Europe, Asia, Africa, and Australia.

Batch Size	Model	Duration (s)	Emissions kg CO ₂	Emissions Rate	CPU Power (W)	GPU Power (W)	RAM Power (W)
1	Lab-MAE	6.415688	4.251868e-08	6.657141e-09	0.50625	0.028650	3.0
	XGBoost	10.866340	1.363608e-06	1.242559e-07	0.21970	0.033817	3.0
32	Lab-MAE	6.993714	2.271253e-07	3.237850e-08	0.257067	0.021300	3.0
	XGBoost	11.703058	2.935091e-06	2.389255e-07	1.908717	0.046033	3.0
64	Lab-MAE	7.826687	5.551631e-07	7.066615e-08	0.722167	0.041750	3.0
	XGBoost	10.946252	1.403389e-06	1.267618e-07	0.278117	0.035150	3.0

tion, while addressing their limitations, particularly in handling temporal dependencies and maintaining performance across diverse patient populations. The significant improvement over XGBoost, especially in complex laboratory parameters, aligns with emerging evidence that properly architected deep learning models can overcome the traditional advantages of tree-based methods in tabular data [van Breugel and van der Schaar \(2024\)](#). However, the observed disparities in performance across racial groups reflect the social patterning of data generation [Teotia et al. \(2024\)](#), where factors such as systemic inequalities in healthcare access contribute to missingness patterns. Addressing this requires not only technical innovations in imputation models but also systemic efforts to improve data equity

4.3. Connection to Foundation Models

The success of Lab-MAE reflects a broader paradigm shift in medical AI, where foundation model architectures are being successfully adapted to specialized clinical tasks. Similar to how large language models have revolutionized natural language processing, our results suggest that transformer-based architectures can effectively capture clinical data’s complex temporal and interdependent nature. The robust performance of Lab-MAE across diverse patient populations suggests that foundation model architectures when properly adapted to clinical domains, can help bridge the gap between general and specialized medical AI applications.

By consolidating multiple tasks into a single, cohesive model, Lab-MAE reduces the redundancy and overhead associated with training and deploying separate models for each feature, as required by XGBoost. This capability is particularly advantageous in healthcare settings like hospitals, where complex

data environments demand robust yet streamlined solutions. Lab-MAE’s foundation model design highlights its potential to adapt effectively to diverse clinical scenarios, offering a powerful combination of scalability and environmental responsibility.

4.4. Limitations and Future Directions

Despite Lab-MAE’s promising results, several limitations merit attention. First, our evaluation was conducted on a single, albeit large, academic medical center dataset, potentially limiting generalizability. Second, while we demonstrated fairness across major demographic groups, future work should investigate intersectional fairness and rare subpopulations. Key directions for future research include: (1) extending Lab-MAE to incorporate structured medical knowledge, (2) investigating transfer learning capabilities across different healthcare settings, and (3) developing interpretability methods specifically designed for temporal clinical predictions.

5. Conclusion

Lab-MAE represents a significant advance in clinical data imputation, demonstrating that foundation model architectures can be effectively adapted for specialized healthcare tasks while maintaining fairness across demographic groups. Our results suggest a promising path forward for developing robust, equitable healthcare AI systems that can handle the complexity of real-world clinical data. As healthcare continues to digitize and generate increasingly complex datasets, approaches like Lab-MAE will be crucial for ensuring both high performance and algorithmic fairness in clinical decision support systems.

Acknowledgments

Acknowledgments Yugang Jia is also affiliated with Verily Life Science LLC.

References

- Peter C Austin, Ian R White, Douglas S Lee, and Stef van Buuren. Missing data in clinical research: a tutorial on multiple imputation. *Canadian Journal of Cardiology*, 37(9):1322–1331, 2021.
- Hangbo Bao, Li Dong, Songhao Piao, and Furu Wei. Beit: Bert pre-training of image transformers. *arXiv preprint arXiv:2106.08254*, 2021.
- David R Bellamy, Bhawesh Kumar, Cindy Wang, and Andrew Beam. Labrador: Exploring the limits of masked language modeling for laboratory data. *arXiv preprint arXiv:2312.11502*, 2023.
- Tianqi Chen and Carlos Guestrin. Xgboost: A scalable tree boosting system. In *Proceedings of the 22nd acm sigkdd international conference on knowledge discovery and data mining*, pages 785–794, 2016.
- Benoit Courty, Victor Schmidt, Goyal-Kamal, MarionCoutarel, Luis Blanche, Boris Feld, inimaz, Jérémy Lecourt, LiamConnell, SabAmine, supatomic, Patrick LLORET, Mathilde Léval, Alexis Cruveiller, Amine Saboni, ouminasara, Franklin Zhao, Aditya Joshi, Christian Bauer, Alexis Bogroff, Hugues de Lavoreille, Niko Laskaris, Alexandre Phiev, Edoardo Abati, rosekelly6400, Douglas Blank, Ziyao Wang, Lucas Otávio, and Armin Catovic. mlco2/codecarbon: v2.8.2, December 2024. URL <https://doi.org/10.5281/zenodo.14518377>.
- Jacob Devlin. Bert: Pre-training of deep bidirectional transformers for language understanding. *arXiv preprint arXiv:1810.04805*, 2018.
- Alexey Dosovitskiy. An image is worth 16x16 words: Transformers for image recognition at scale. *arXiv preprint arXiv:2010.11929*, 2020.
- Tianyu Du, Luca Melis, and Ting Wang. Remasker: Imputing tabular data with masked autoencoding. *arXiv preprint arXiv:2309.13793*, 2023.
- Léo Grinsztajn, Edouard Oyallon, and Gaël Varoquaux. Why do tree-based models still outperform deep learning on typical tabular data? *Advances in neural information processing systems*, 35:507–520, 2022.
- Kaiming He, Xinlei Chen, Saining Xie, Yanghao Li, Piotr Dollár, and Ross Girshick. Masked autoencoders are scalable vision learners. In *Proceedings of the IEEE/CVF conference on computer vision and pattern recognition*, pages 16000–16009, 2022.
- Alistair Johnson, Lucas Bulgarelli, Tom Pollard, Steven Horng, Leo Anthony Celi, and Roger Mark. Mimic-iv. *PhysioNet*. Available online at: <https://physionet.org/content/mimiciv/1.0/> (accessed August 23, 2021), pages 49–55, 2020.
- Alistair EW Johnson, Lucas Bulgarelli, Lu Shen, Alvin Gayles, Ayad Shammout, Steven Horng, Tom J Pollard, Sicheng Hao, Benjamin Moody, Brian Gow, et al. Mimic-iv, a freely accessible electronic health record dataset. *Scientific data*, 10(1): 1, 2023.
- Arlind Kadra, Marius Lindauer, Frank Hutter, and Josif Grabocka. Well-tuned simple nets excel on tabular datasets. *Advances in neural information processing systems*, 34:23928–23941, 2021.
- Diederik P Kingma. Auto-encoding variational bayes. *arXiv preprint arXiv:1312.6114*, 2013.
- Ibna Kowsar, Shourav B Rabbani, and Manar D Samad. Attention-based imputation of missing values in electronic health records tabular data. In *2024 IEEE 12th International Conference on Healthcare Informatics (ICHI)*, pages 177–182. IEEE, 2024.
- Rayan Krishnan, Pranav Rajpurkar, and Eric J Topol. Self-supervised learning in medicine and healthcare. *Nature Biomedical Engineering*, 6(12): 1346–1352, 2022.
- Do-Hoon Lee and Han-joon Kim. A self-attention-based imputation technique for enhancing tabular data quality. *Data*, 8(6):102, 2023.
- Jiang Li, Xiaowei S Yan, Durgesh Chaudhary, Venkatesh Avula, Satish Mudiganti, Hannah Husby, Shima Shahjouei, Ardavan Afshar, Walter F Stewart, Mohammed Yeasin, et al. Imputation of missing values for electronic health record laboratory data. *NPJ digital medicine*, 4(1):147, 2021.

- Yuan Luo. Evaluating the state of the art in missing data imputation for clinical data. *Briefings in Bioinformatics*, 23(1):bbab489, 2022.
- Yuan Luo, Peter Szolovits, Anand S Dighe, and Jason M Baron. Using machine learning to predict laboratory test results. *American journal of clinical pathology*, 145(6):778–788, 2016.
- Victor M Panaretos and Yoav Zemel. Statistical aspects of wasserstein distances. *Annual review of statistics and its application*, 6(1):405–431, 2019.
- Arshi Parvaiz, Muhammad Anwaar Khalid, Rukhsana Zafar, Huma Ameer, Muhammad Ali, and Muhammad Moazam Fraz. Vision transformers in medical computer vision—a contemplative retrospection. *Engineering Applications of Artificial Intelligence*, 122:106126, 2023.
- Pawel Renc, Yugang Jia, Anthony E Samir, Jaroslaw Was, Quanzheng Li, David W Bates, and Arkadiusz Sitek. Zero shot health trajectory prediction using transformer. *NPJ Digital Medicine*, 7(1):256, 2024.
- Richard D Riley, Lucinda Archer, Kym IE Snell, Joie Ensor, Paula Dhiman, Glen P Martin, Laura J Bonnett, and Gary S Collins. Evaluation of clinical prediction models (part 2): how to undertake an external validation study. *bmj*, 384, 2024.
- CodeCarbon Team. Global energy mix data, 2024. URL https://github.com/mlco2/codecarbon/blob/master/codecarbon/data/private_infra/global_energy_mix.json. Accessed: December 25, 2024.
- Khushboo Teotia, Yueran Jia, Naira Link Woite, Leo Anthony Celi, João Matos, and Tristan Struja. Variation in monitoring: Glucose measurement in the icu as a case study to preempt spurious correlations. *Journal of Biomedical Informatics*, 153:104643, 2024.
- Boris van Breugel and Mihaela van der Schaar. Why tabular foundation models should be a research priority. *arXiv preprint arXiv:2405.01147*, 2024.
- A Vaswani. Attention is all you need. *Advances in Neural Information Processing Systems*, 2017.
- Cédric Villani and Cédric Villani. The wasserstein distances. *Optimal transport: old and new*, pages 93–111, 2009.
- Akbar K Waljee, Ashin Mukherjee, Amit G Singal, Yiwei Zhang, Jeffrey Warren, Ulysses Balis, Jorge Marrero, Ji Zhu, and Peter DR Higgins. Comparison of imputation methods for missing laboratory data in medicine. *BMJ open*, 3(8):e002847, 2013.
- Richard Wu, Aoqian Zhang, Ihab Ilyas, and Theodoros Rekatsinas. Attention-based learning for missing data imputation in holoclean. *Proceedings of Machine Learning and Systems*, 2:307–325, 2020.
- Davina J Zamanzadeh, Panayiotis Petousis, Tyler A Davis, Susanne B Nicholas, Keith C Norris, Katherine R Tuttle, Alex AT Bui, and Majid Sarrafzadeh. Autopopulus: a novel framework for autoencoder imputation on large clinical datasets. In *2021 43rd Annual International Conference of the IEEE Engineering in Medicine & Biology Society (EMBC)*, pages 2303–2309. IEEE, 2021.
- Xinmeng Zhang, Chao Yan, Cheng Gao, Bradley A Malin, and You Chen. Predicting missing values in medical data via xgboost regression. *Journal of healthcare informatics research*, 4:383–394, 2020.

Appendix A. Performance metrics

Evaluation Metrics: The following metrics were used to measure the accuracy of the predictions for each lab value:

- **RMSE:** Represents the square root of the average squared differences between the predicted and actual values, emphasizing larger errors.

$$\text{RMSE} = \sqrt{\frac{1}{n} \sum_{i=1}^n (y_i - \hat{y}_i)^2} \quad (5)$$

where n is the number of data points, y_i represents the true values, and \hat{y}_i represents the predicted values.

- **R^2 :** Evaluates the proportion of variance in the dependent variable that can be explained by the model, with values closer to 1 indicating a stronger predictive capability.

$$R^2 = 1 - \frac{\sum_{i=1}^n (y_i - \hat{y}_i)^2}{\sum_{i=1}^n (y_i - \bar{y})^2} \quad (6)$$

where \bar{y} is the mean of the observed data, y_i represents the true values, and \hat{y}_i represents the predicted values.

- **Wasserstein Distance:** WD measures the distance between two probability distributions [Villani and Villani \(2009\)](#). It is particularly sensitive to differences in the tails of distributions, making it a suitable for capturing the ability of the model to predict abnormal values [Panaretos and Zemel \(2019\)](#). Given two distributions P (actual values) and Q (predicted values), the 1st Wasserstein distance is defined as:

$$W(P, Q) = \inf_{\gamma \in \Gamma(P, Q)} \int_{\mathbb{R}^2} \|x - y\| d\gamma(x, y) \quad (7)$$

where $\Gamma(P, Q)$ represents the set of all joint distributions with marginals P and Q . In our implementation, WD is approximated using the cumulative distribution functions (CDFs) of the predicted and actual values:

$$W(P, Q) \approx \int_{-\infty}^{\infty} |F_P(x) - F_Q(x)| dx \quad (8)$$

where $F_P(x)$ and $F_Q(x)$ are the CDFs of the actual and predicted distributions, respectively.

This systematic evaluation allowed for a direct comparison of the Lab-MAE and XGBoost models, highlighting their relative strengths and weaknesses in accurately imputing missing lab values in the medical dataset. The consistent use of the same test data points for both models ensured a fair and unbiased evaluation of their performance in this critical imputation task.

Appendix B. Carbon footprint measurement

B.1. Methods: Carbon footprint measurement

The total emissions E were calculated using [Courty et al. \(2024\)](#) as:

$$E = \int_0^T P(t) dt \quad (9)$$

where $P(t)$ is the power consumption at time t , and T is the total runtime. Power consumption was derived as:

$$P(t) = P_{\text{CPU}}(t) + P_{\text{GPU}}(t) + P_{\text{RAM}}(t) \quad (10)$$

The energy consumption E_{consumed} is calculated as:

$$E_{\text{consumed}} = \sum_{i=1}^n (P_{\text{CPU}} \times t_i + P_{\text{GPU}} \times t_i + P_{\text{RAM}} \times t_i) \quad (11)$$

Carbon emissions Emissions are then computed as:

$$\text{Emissions} = E_{\text{consumed}} \times \text{EmissionFactor} \quad (12)$$

where EmissionFactor depends on the energy grid of the location, accounting for the carbon intensity of electricity. The information of the EmissionFactor per country is available in [Team \(2024\)](#).

B.2. Results: Carbon footprint measurement

Table 4: Carbon Emissions and Power Usage for Batch Size 1

Continent	Model	Duration (s)	Emissions (kg CO ₂)	Emissions Rate	CPU Power (W)	GPU Power (W)
Africa	Lab-MAE	6.35	4.85×10^{-9}	7.63×10^{-10}	0.22	0.00
Africa	XGBoost	10.67	1.82×10^{-7}	1.71×10^{-8}	0.32	0.00
Asia	Lab-MAE	6.33	4.92×10^{-8}	7.77×10^{-9}	0.12	0.00
Asia	XGBoost	10.82	2.63×10^{-6}	2.43×10^{-7}	0.29	0.05
Australia	Lab-MAE	6.41	1.05×10^{-7}	1.63×10^{-8}	0.63	0.10
Australia	XGBoost	11.28	2.54×10^{-6}	2.25×10^{-7}	0.33	0.11
Europe	Lab-MAE	6.66	8.27×10^{-9}	1.24×10^{-9}	0.26	0.07
Europe	XGBoost	10.74	2.15×10^{-7}	2.00×10^{-8}	0.06	0.00
North America	Lab-MAE	6.41	4.23×10^{-8}	6.59×10^{-9}	0.50	0.00
North America	XGBoost	11.01	1.64×10^{-6}	1.48×10^{-7}	0.27	0.05
South America	Lab-MAE	6.33	4.59×10^{-8}	7.26×10^{-9}	1.31	0.00
South America	XGBoost	10.68	9.82×10^{-7}	9.20×10^{-8}	0.05	0.00

Table 5: Carbon Emissions and Power Usage for Batch Size 32

Continent	Model	Duration (s)	Emissions (kg CO ₂)	Emissions Rate	CPU Power (W)	GPU Power (W)
Africa	Lab-MAE	7.02	2.96×10^{-8}	4.22×10^{-9}	0.07	0.02
Africa	XGBoost	10.95	1.82×10^{-7}	1.66×10^{-8}	0.10	0.02
Asia	Lab-MAE	6.94	3.77×10^{-7}	5.44×10^{-8}	0.06	0.00
Asia	XGBoost	12.76	1.10×10^{-5}	8.62×10^{-7}	8.37	0.14
Australia	Lab-MAE	7.09	4.35×10^{-7}	6.14×10^{-8}	0.15	0.10
Australia	XGBoost	11.95	3.17×10^{-6}	2.66×10^{-7}	0.60	0.10
Europe	Lab-MAE	6.93	3.55×10^{-8}	5.13×10^{-9}	0.17	0.00
Europe	XGBoost	12.42	4.30×10^{-7}	3.46×10^{-8}	1.67	0.01
North America	Lab-MAE	7.06	3.24×10^{-7}	4.59×10^{-8}	1.04	0.01
North America	XGBoost	11.22	1.64×10^{-6}	1.46×10^{-7}	0.24	0.00
South America	Lab-MAE	6.94	1.61×10^{-7}	2.32×10^{-8}	0.06	0.00
South America	XGBoost	10.92	1.19×10^{-6}	1.09×10^{-7}	0.47	0.00

 Table 6: Carbon Emissions and Power Usage for
Batch Size 64

Continent	Model	Duration (s)	Emissions (kg CO ₂)	Emissions Rate	CPU Power (W)	GPU Power (W)
Africa	Lab-MAE	7.85	6.33×10^{-8}	8.07×10^{-9}	0.13	0.00
Africa	XGBoost	10.70	1.92×10^{-7}	1.79×10^{-8}	0.45	0.00
Asia	Lab-MAE	7.87	1.23×10^{-6}	1.56×10^{-7}	1.07	0.10
Asia	XGBoost	11.20	2.94×10^{-6}	2.63×10^{-7}	0.36	0.10
Australia	Lab-MAE	7.88	8.91×10^{-7}	1.13×10^{-7}	0.35	0.10
Australia	XGBoost	11.07	2.45×10^{-6}	2.21×10^{-7}	0.20	0.10
Europe	Lab-MAE	7.70	7.82×10^{-8}	1.02×10^{-8}	0.24	0.04
Europe	XGBoost	10.76	2.34×10^{-7}	2.18×10^{-8}	0.31	0.00
North America	Lab-MAE	7.83	4.99×10^{-7}	6.38×10^{-8}	0.10	0.01
North America	XGBoost	11.03	1.52×10^{-6}	1.38×10^{-7}	0.13	0.00
South America	Lab-MAE	7.83	5.73×10^{-7}	7.32×10^{-8}	2.44	0.00
South America	XGBoost	10.93	1.08×10^{-6}	9.85×10^{-8}	0.21	0.00

Appendix C. Impact of shortcut features

C.1. Methods: Impact of follow-up data as a shortcut feature

In addition to analyzing fairness across races, we also examined the Lab-MAE model’s performance in scenarios where follow-up data was present versus when it was absent. This analysis aimed to understand if the availability of follow-up data serves as a shortcut feature, potentially inflating the model’s performance by providing additional context.

For this analysis, the following procedure was adopted:

- For each lab value, we identified the corresponding follow-up values (denoted as `npval_last`) and separated the test samples into two groups: those with follow-up values and those without.
- The imputation model’s performance was then evaluated separately for each group to determine how the presence or absence of follow-up data affected its predictive performance of the model on data imputation.
- Metrics such as WD, and R^2 were calculated for each group to quantify the performance variations between the two scenarios.

This experiment allowed us to observe whether the model’s predictive performance disproportionately relies on the availability of follow-up data, which could lead to biased predictions when such data is not present.

The findings from both the fairness analysis across racial groups and the follow-up data evaluation are crucial for understanding the Lab-MAE model’s robustness and its potential biases. This analysis also aids in identifying areas where the model could be further improved to ensure more equitable performance across diverse patient populations.

C.2. Results: Impact of follow-up data as a shortcut feature

In this section, we analyze the impact of the Lab-MAE and XGBoost models to shortcuts by comparing their imputation performance with and without the presence of follow-up values. Follow-up values represent additional lab measurements taken after the initial test, providing a temporal context that

could serve as a shortcut for predicting the target lab values.

To do so, we evaluated the performance of both models using the R^2 metrics for the lab values with and without follow-up data. The comparison of the distributions for each lab value and the WD values is available in the supplementary materials.

Table 7: Comparison of Lab-MAE and XGBoost models with and without follow-up values for imputation.

Model	Follow-Up	R^2
XGBoost	✓	0.7391
		0.6089
Lab-MAE	✓	0.7661
		0.6544

As illustrated in Table 7, both models experience a noticeable decline in performance when follow-up values are absent. The R^2 values reflect a decrease in model performance without follow-up values. For XGBoost, R^2 drops from 0.7391 with follow-up to 0.6089 without follow-up. Lab-MAE shows a similar pattern, with R^2 declining from 0.7661 with follow-up to 0.6544 without. These results suggest that both models benefit significantly from the additional temporal information provided by follow-up values.

The Lab-MAE model outperforms XGBoost across both scenarios, demonstrating a smaller reduction in accuracy when follow-up values are excluded. This indicates that the Lab-MAE model is more robust in handling cases where only the initial lab value is available, further highlighting the effectiveness of its Transformer-based architecture in capturing complex patterns even with limited data.

Appendix D. R2 metrics comparison

D.1. R2 metrics comparison of Lab-MAE vs XGBoost for the top 20 lab values

Figure 2 provides a visual representation of the performance metrics for the top 20 lab values, highlighting the consistent improvement of the Lab-MAE model over XGBoost. This visual analysis further supports the numerical results, emphasizing the Lab-MAE model’s enhanced ability to predict missing lab values accurately.

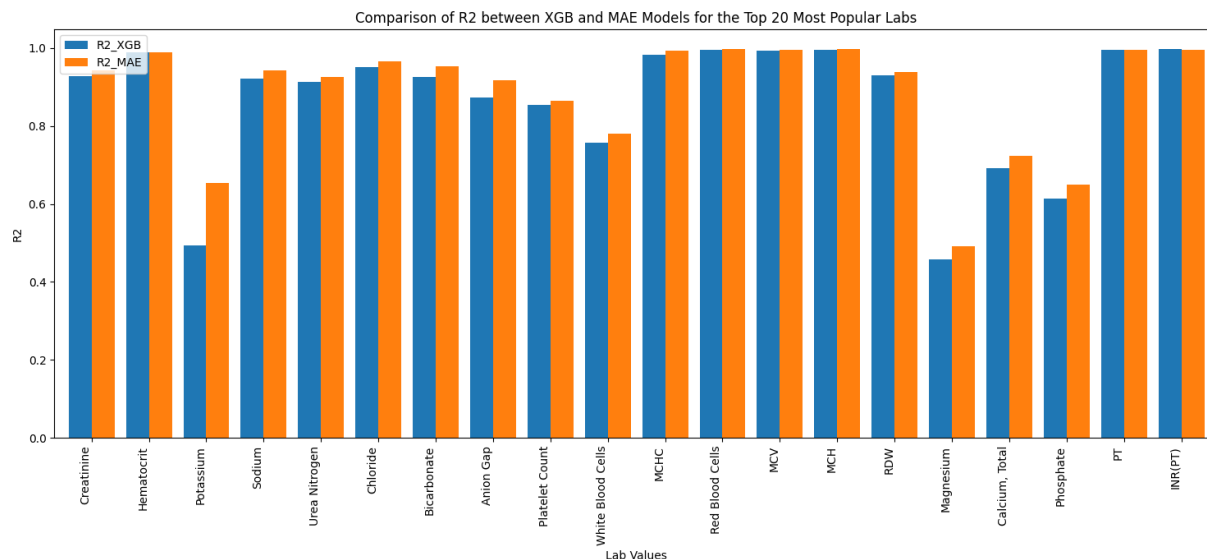


Figure 2: Comparison of R^2 between Lab-MAE and XGBoost models for the top 20 lab values. Orange is our Lab-MAE model and blue is XGBoost

D.2. R2 metrics comparison per race of Lab-MAE for the top 20 lab values

Figure 3 visually depicts the variation in R^2 scores for the top 20 lab values across different racial groups. This visualization clearly demonstrates the disparities in model performance, with certain lab values consistently showing higher predictive accuracy for specific races while underperforming for others.

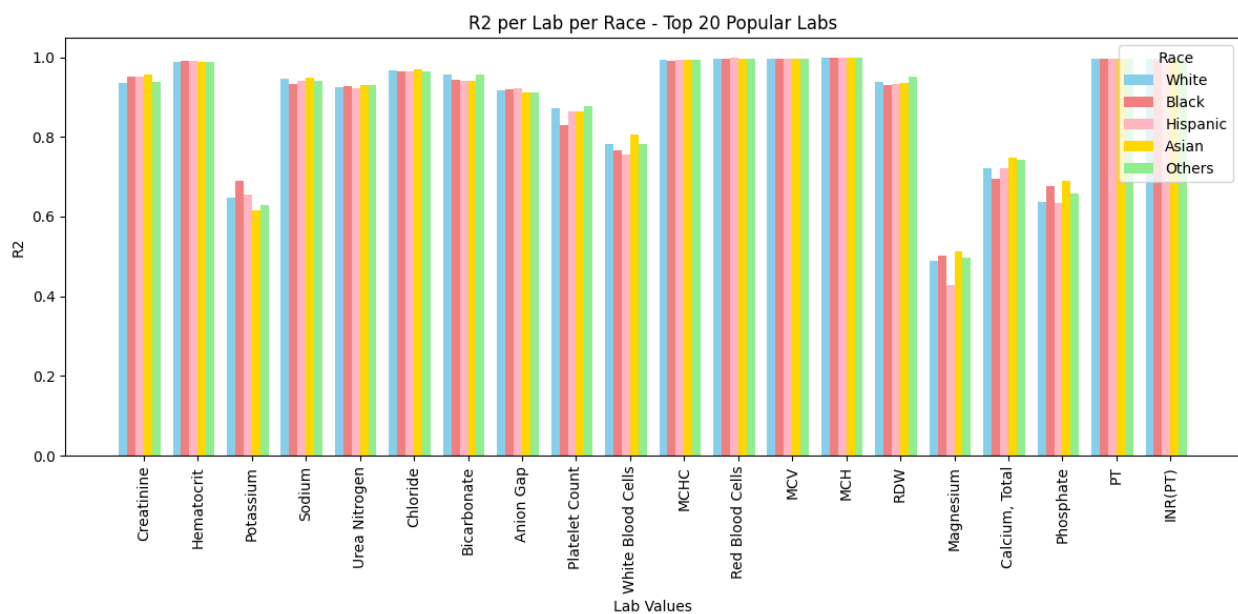


Figure 3: Comparison of the Lab-MAE model’s performance across different races for the top 20 lab values. Blue indicates White race, red indicates black race, pink indicates Hispanic, yellow indicates Asian, and green indicates others.

Appendix E. Performance metrics across races

Table 8: Performance metrics (R^2) of Lab-MAE model across different racial groups for the top 20 lab values. The best-performing race for each lab value is highlighted in bold.

Lab ID	Asian	Black	Hispanic	Others	White
Anion Gap	0.9105	0.9197	0.9223	0.9110	0.9181
Bicarbonate	0.9419	0.9431	0.9412	0.9577	0.9562
Calcium, Total	0.7479	0.6950	0.7211	0.7439	0.7211
Chloride	0.9702	0.9653	0.9647	0.9651	0.9671
Creatinine	0.9565	0.9525	0.9522	0.9384	0.9354
Glucose	0.4143	0.4669	0.4700	0.4823	0.4637
Magnesium	0.5134	0.5028	0.4278	0.4965	0.4888
Phosphate	0.6892	0.6773	0.6336	0.6581	0.6366
Potassium	0.6151	0.6891	0.6566	0.6290	0.6487
Sodium	0.9488	0.9327	0.9418	0.9397	0.9453
Urea Nitrogen	0.9307	0.9276	0.9232	0.9313	0.9235
Hematocrit	0.9884	0.9911	0.9910	0.9885	0.9889
Hemoglobin	0.9983	0.9981	0.9985	0.9981	0.9983
MCH	0.9982	0.9979	0.9975	0.9978	0.9977
MCHC	0.9941	0.9922	0.9923	0.9936	0.9945
MCV	0.9962	0.9966	0.9954	0.9958	0.9955
Platelet Count	0.8654	0.8310	0.8644	0.8772	0.8712
RDW	0.9365	0.9288	0.9334	0.9522	0.9381
Red Blood Cells	0.9966	0.9964	0.9979	0.9968	0.9974
White Blood Cells	0.8061	0.7672	0.7559	0.7822	0.7828

Table 9: Performance metrics (WD) of Lab-MAE model across different racial groups for the top 20 lab values. The best-performing race for each lab value is highlighted in bold.

Lab ID	Asian	Black	Hispanic	Others	White
Anion Gap	0.2159	0.2147	0.2011	0.2216	0.2058
Bicarbonate	0.2126	0.2124	0.2071	0.2033	0.1944
Calcium, Total	0.0872	0.0903	0.0890	0.0755	0.0818
Chloride	0.2360	0.2387	0.2338	0.2330	0.2269
Creatinine	0.0408	0.0471	0.0393	0.0360	0.0336
Glucose	9.6687	11.1270	11.6503	10.5412	9.6597
Hematocrit	0.0502	0.0423	0.0460	0.0455	0.0404
Hemoglobin	0.0287	0.0272	0.0273	0.0267	0.0260
MCH	0.0325	0.0297	0.0298	0.0307	0.0289
MCHC	0.0291	0.0286	0.0283	0.0273	0.0279
MCV	0.2389	0.2313	0.2411	0.2374	0.2402
Magnesium	0.0731	0.0710	0.0692	0.0686	0.0718
Phosphate	0.1378	0.1513	0.1588	0.1604	0.1572
Platelet Count	8.8684	7.3407	7.2225	6.7014	7.7651
Potassium	0.0926	0.0965	0.1005	0.0969	0.0954
RDW	0.0829	0.0874	0.0920	0.0633	0.0703
Red Blood Cells	0.0059	0.0050	0.0048	0.0046	0.0042
Sodium	0.2176	0.2292	0.2276	0.2265	0.2167
Urea Nitrogen	0.6366	0.9511	0.6031	0.5351	0.5394
White Blood Cells	0.4670	0.5065	0.4525	0.4512	0.4537

Table 10: Performance metrics (RMSE) of Lab-MAE model across different racial groups for the top 20 lab values. The best-performing race for each lab value is highlighted in bold.

Lab ID	Asian	Black	Hispanic	Others	White
Anion Gap	0.8643	0.8356	0.7685	0.8601	0.7936
Bicarbonate	0.8140	0.8678	0.8152	0.7607	0.7375
Calcium, Total	0.3175	0.3435	0.3257	0.3192	0.3202
Chloride	0.8745	0.9261	0.9079	0.9201	0.8565
Creatinine	0.2467	0.2609	0.2293	0.2351	0.2239
Glucose	30.9953	31.3567	32.5657	30.1562	28.1981
Hematocrit	0.6032	0.5263	0.5282	0.5753	0.5719
Hemoglobin	0.0805	0.0848	0.0750	0.0822	0.0779
MCH	0.1042	0.1109	0.1137	0.1089	0.1080
MCHC	0.1095	0.1267	0.1257	0.1148	0.1092
MCV	0.3992	0.3792	0.4068	0.4038	0.4075
Magnesium	0.1779	0.1783	0.1822	0.1763	0.1778
Phosphate	0.5058	0.5182	0.5311	0.5104	0.5073
Platelet Count	40.3788	41.9516	39.3368	38.1394	39.6089
Potassium	0.2790	0.2724	0.2745	0.2779	0.2680
RDW	0.5790	0.5828	0.5794	0.4920	0.5472
Red Blood Cells	0.0401	0.0414	0.0317	0.0368	0.0335
Sodium	0.8878	0.9470	0.8905	0.9367	0.8559
Urea Nitrogen	4.7031	4.8157	4.5611	4.3308	4.4837
White Blood Cells	1.9842	1.9612	1.9424	1.9685	1.9190

Appendix F. Lab value distribution of Lab-MAE and XGBoost

Prediction vs real distributions in test set [\[here\]](#)

Appendix G. Lab value distributions per race

- Prediction vs real distributions per race for Lab-MAE model in test set [\[here\]](#)
- Prediction vs real distributions per race for XGBoost model in test set [\[here\]](#)

Appendix H. Lab value distributions with vs without follow-up values

- Prediction vs real distributions with vs without follow-up value in test set for Lab-MAE [\[here\]](#)
- Prediction vs real distributions with vs without follow-up value in test set for XGBoost [\[here\]](#)